ABSTRACT

Testing of New Front-End Electronics for the Hadron Calorimeter at CERN

John Lawrence

Director: Kenichi Hatakeyama, Ph.D.

The Hadron Calorimeter (HCAL), a major component of the Compact Muon Solenoid (CMS) detector at CERN, is designed to detect hadrons produced in proton-proton collisions supplied by the Large Hadron Collider (LHC). The HCAL is currently being upgraded with new readout modules that contain Silicon Photomultipliers (SiPMs), photodetectors that accept light from scintillator tiles and convert them to charge signals. Using a test beam capable of producing the same types of particles measured in the CMS detector, the new readout modules were tested in conditions like those of the CMS detector to fully understand their functionality before installation. Since the SiPMs in the new readout modules process the signals very differently than the hybrid photodiodes in the old readout modules, the analysis of test beam data provides insight into the features of the SiPMs. A virtual SiPM simulation was also created to assist in the analysis.

APPROVED BY DIRECTOR OF HONORS THESIS:

____

Dr. Kenichi Hatakeyama, Department of Physics

APPROVED BY THE HONORS PROGRAM:

____

Dr. Elizabeth Corey, Director

DATE: ____________________

TESTING OF NEW FRONT-END ELECTRONICS FOR THE HADRON CALORIMETER AT CERN

A Thesis Submitted to the Faculty of

Baylor University

In Partial Fulfillment of the Requirements for the

Honors Program

By

John Lawrence

Waco, Texas

May 2018

TABLE OF CONTENTS

LIST OF FIGURES

CHAPTER ONE

Basic Particle Physics and CERN

Ever since ancient Greece people have been trying to discover what makes up everything. Back then they said that everything was comprised of four elements: earth, fire, water, and air. Although modern scientists use more than four elements, they are still trying to categorize the most fundamental element that makes up everything. Democritus, an ancient Greek scientist, proposed that everything if divided enough times could be broken down into atoms at their most fundamental object. While some people names something the atom that was not the most fundamental substance, scientists today are still pursuing the "atom" theorized by Democritus, the most fundamental substance.

In the 19th century John Dalton believed he found the most fundamental particle and named it the atom, but as time passed, there was strong evidence that even atoms had internal components and structure. This was proven when J. J. Thompson in the late 19th century found the electron, which proved to be a component of the atom. This was not only the first fundamental particle discovered, but also the beginning of particle physics as a field of study. While it was an insightful discovery that led to many inventions, there were still many unknowns about the atom. About a decade after Thompson, Robert Millikan made fine measurements of the charge and mass of the electron, but this raised even more questions about the atom. It was not until Ernest Rutherford in the early 20th century showed that the atom is mostly empty space with a very dense core called the nucleus which has an opposite charge to that of the electron. He did this by shooting alpha particles, made up of two protons and two neutrons, at gold foil and observing their scattering angle. In this experiment most of the alpha particles passed through unperturbed while a handful were majorly deflected. From this observation, Rutherford concluded that most of the atom was empty space while having a highly dense core called the nucleus.

These discoveries showed there were more things to explore past the atom, and in parallel there were equally important theories being developed. Quantum mechanics is essential to the study of sub-atomic particles as they no longer behave according to classical mechanics. During this development Max Planck was doing his work on the quantization of energy. This set the groundwork for quantum mechanics and also served as a basis to Einstein's work. In 1905, Einstein formulated his theory of special relativity, which had several major impacts on the field of particle physics. One of the most important was quantization of light into particles called photons. Although light had long been thought of as a wave, Einstein showed many of its particle-like properties leading to the wave-particle duality of light. Eventually Louis De Brogile extended this duality to all particles theorizing that all particles including electrons and other sub-atomic particles could be described using waves or particles.

Einstein's theory of relativity had another major impact on particle physics. Probably the most famous of Einstein's equation, $E = mc^2$, shows the mass-energy relationship. One of the implications of quantum mechanics is that if something can happen it will happen under a certain probability. This means that given the right conditions and enough energy one can simply create mass. There are other conservation laws which need to be followed and which are still relevant to particle physics, but conservation of energy is one of the biggest limiters as it says to create more massive particles more energy is needed.

As these theories became more complete, they allowed for the further description of sub-atomic particles, like the states of the electrons in the atoms and the protons and neutrons that make up the nucleus of the atom. Scientist also began to find evidence of fundamental particles not in atoms. In 1932 Carl Anderson found evidence of a muon from cosmic rays. In addition, as scientists began to probe higher energies they found evidence of internal structure within protons and neutrons. In 1968 at the Standford Linear Accelerator Center, they found evidence of particles within protons and neutrons, which were later called quarks.

The discovery of more and more fundamental particles led to the formulation of the standard model. Part of the standard model included something like a periodic table for fundamental particles. The two main groups of particles on the standard model are fermions, which have half integer spin, and bosons, which have integer spin. The main physical difference this causes is from the Pauli exclusion principle, which allows fermions to build into larger arrangements. Because of this fermions are the building blocks of the macroscopic world as they make up protons neutrons, and atoms.

As shown in table 1.1 there are several different groups of particles in the standard model. The first group is a sub-category of fermions called quarks. The main factor that distinguishes quarks from other fundamental fermions is that they interact via the strong force. While they also interact via the electromagnetic and weak force, the strong force is the more dominate one. Quarks can exist in isolation only for a short time, but rather exist in groups of two three or possibly more. When three quarks form a particle it is called a baryon. A proton which is made up of two up and one down quarks and a neutron which is made up of two down and one up quarks are both baryons. Each of the quarks inside a baryon has a different color red, green, or blue which serves as the "charge" for the strong force. Like electric charge strong force color attracts other colors and repels similar, but since the baryon has one of each it has a net color of white or nothing. In addition to the six flavors of quark listed on table 1.1, there is also a corresponding anti-quark with the same properties but opposite charge and color. Quarks can also form in pairs called mesons, which have a quark and anti-quark. If one tries to separate the individual quarks from the respective baryons or mesons the energy required to separate them is more than the energy required to simply create more quarks. For instance, when a proton is separated into its constituent quarks the necessary input energy would rather create new quarks forming baryons and mesons, leaving no quark in isolation.

The other category of fermionic particles are the leptons. Unlike the quarks, leptons are not affected by the strong force, and therefore it is more common to find them in isolation. The electron is the most well-known lepton, but there are also two other flavors which are heavier copies of the electron. As with all of the particles on the standard model, there are corresponding anti-particles for the each lepton with the same mass but opposite charge. In addition to the three charged leptons, there are also three neutral leptons which are called neutrinos. Each one has a charged lepton pair. Neutrinos are nearly mass-less and do not have any charge. Since the only force that affects them is the weak force, they have a very low probability of interaction. This means that they essentially pass through everything without interaction. Although they do interact through processes like beta decay, most neutrinos simply just travel through everything.

Finally, there are the bosons. Bosons are different from both leptons and quarks in that they have integer spin, but the individual bosons differ from each other in which fundamental force affects them. While leptons and quarks combine together to form complex arrangements such as atoms and all of matter, bosons serve as the force carriers. The photon serves as the mediator for the electromagnetic force. This means that whenever two electrons repel each other there is a photon to mediate that interaction. The strong force interaction is mediated by the gluon. The weak force is mediated by the W boson, for those interactions with changes in charge, and the Z boson, for those interaction with no changes in charge.

One nice aspect about the standard model is that it gives this convenient table of fundamental particles, but the discovery all of these particles was not simple. The electron is the only particle in the standard model that is found in isolation at energies

Table 1.1. Particles on the Standard Model

Particle Type	Name	Charge	Mass	Spin
Quarks	Up	$+2/3$	$2.2\,\mathrm{MeV}/c^2$	$\pm 1/2$
	Down	$-1/3$	$4.7\,\mathrm{MeV}/c^2$	$\pm 1/2$
	Charm	$+2/3$	$1.28\,\mathrm{GeV}/c^2$	$\pm 1/2$
	Strange	$-1/3$	$96\,\mathrm{MeV}/c^2$	$\pm 1/2$
	Top	$+2/3$	$173.1\,\mathrm{GeV}/c^2$	$\pm 1/2$
	Bottom	$-1/3$	$4.18\,\mathrm{GeV}/c^2$	$\pm 1/2$
Leptons	Electron	-1	$0.511\,\mathrm{MeV}/c^2$	$\pm 1/2$
	Muon	-1	$105.7\,\mathrm{MeV}/c^2$	$\pm 1/2$
	Tau	-1	$1.776\,\mathrm{GeV}/c^2$	$\pm 1/2$
	Electron Neutrino	0	≈ 0	$\pm 1/2$
	Muon Neutrino	0	≈ 0	$\pm 1/2$
	Tau Neutrino	0	≈ 0	$\pm 1/2$
Gauge Bosons	Photon	0	0	± 1
	Gluon	0	0	± 1
	W boson	± 1	$80.4\,\mathrm{GeV}/c^2$	± 1
	Z boson	0	$91.19\,\mathrm{GeV}/c^2$	± 1
Scalar Boson	Higgs Boson	0	$125.1\,\mathrm{GeV}/c^2$	0

used on earth. To find the next particle, the muon, scientist had to look at cosmic rays, which provided the energy needed to create these particles. While neutrinos are plentiful they interact so infrequently scientist are still struggling to create an efficient detector for them. To discover the remaining particles in the standard model, they had to use particle colliders. Throughout the last few decades, scientists have built colliders to probe higher and higher energies, in order to make them capable of discovering more fundamental particles. In 2012, using the Large Hadron Collider at CERN scientists were able to find evidence of the Higgs boson, the final particle in the standard model. Data showing evidence of the Higgs boson is shown in figure 1.1. However, there are still phenomenon in the universe that cannot be explained using the standard model, such as gravity and dark matter. There are several theories beyond the standard model that offer explanations for these, but they also say there

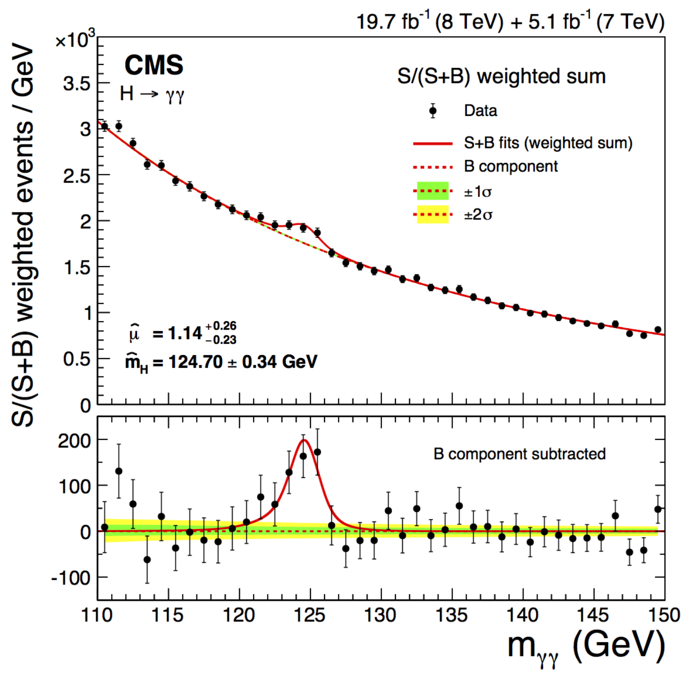

Figure 1.1. Data showing evidence of the Higgs Boson from a two photon decay [1].

are more fundamental particles to be discovered at higher energies. This is one of the main goals of the LHC experiment.

After an upgrade that ended in 2015 the LHC is now capable of producing particle collisions never before achieved. The LHC has also increased its rate of collisions. To be able to gather usable data from these higher energies and collision rates the detectors on the LHC need to be upgraded as well. The Compact Muon Solenoid (CMS), one of the detectors on the LHC, is currently undergoing several upgrades. Chapter 2 will discuss the details of the LHC and the CMS detector. Chapters 4 and 3 will discuss the work I did for the CMS detector outlining the analysis done on new electronics that were installed in the detector during the winter of 2018 as apart of the upgrades

CHAPTER TWO

Large Hadron Collider and Compact Muon Solenoid

2.1 The Large Hadron Collider

The LHC is located at CERN near Geneva, Switzerland. It has a circular shape and is 27 kilometers in circumference. It is about 100 meters underground and as shown in 2.1 it simply goes under the towns and farmland in the area. To look for undiscovered particles, the LHC collides protons at high energies. After the recent upgrade the LHC now collides protons with a center of mass energy of 13 TeV, meaning the individual protons each have 6.5 TeV of energy. The theory of special relativity says that a particle can only approach the speed of light. As the protons in the LHC are traveling close to the speed of light it is more useful to use their energy rather than their speed. In addition, mass is often put into units of energy of the speed of light squared making the mass to energy conversion simple.

The process the LHC uses sounds simple when put into common terms. It accelerated protons to speeds very close to the speed of light and collides them in the center of a detector to see what comes out of these collisions. However actually accomplishing this is not simple at all. To start this entire process electrons are stripped off of hydrogen gas supplying the protons for the LHC. After this, the protons are put into a series of different accelerator each designed to accelerator the protons to higher and higher energies. The first accelerator is the Linac2 linear accelerator, which pushes the protons up to 50 MeV. Then they are sent to the Proton Synchrotron Booster which can push them to 1.4 GeV, after which the Proton Synchrotron ring accelerates the protons to 25 GeV. At this point the protons are sorted to control the frequency at which the collisions will occur. The protons are sorted into bunches such that a proton bunch passes by every 25ns. Each bunch has about 100 billion protons

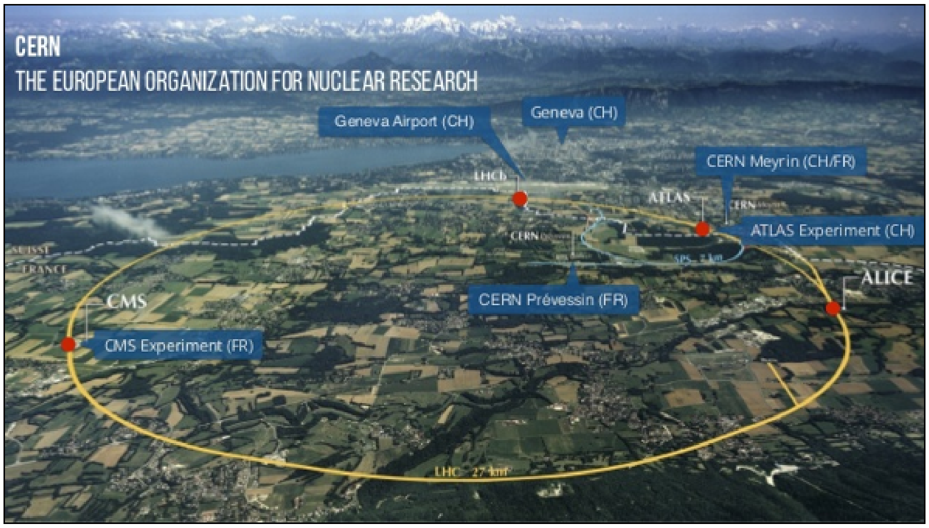

Figure 2.1. A picture of the LHC (outlined in yellow) with the different detectors highlighted

in it. After sorted into these bunches, the protons are sent to the Super Proton Synchrotron where they achieve an energy of 450 GeV. Finally, the protons are fed into the LHC where they will be accelerated to their highest energy. An illustration of all of these accelerators is shown in figure 2.2.

When the LHC has accelerated its particles to its peak energy it collides the particles in the middle of four different detectors. LHCb, ALICE, ATLAS, and CMS are the names of the four detectors that were built to study collisions supplied by the LHC. The CMS detector is the one I worked on during my undergraduate career, and is discussed in detail below.

2.2 The CMS Detector

The CMS detector is designed to detector particles coming out of the proton-proton collisions supplied by the LHC [2]. As collisions produce many types of particles, the CMS detector is split up into several different sub-detectors. Starting at the closest to the collision point outward, first is the silicon tracker. The Silicon Tracker is capable of finely measuring the path of the particles that travel through it. The

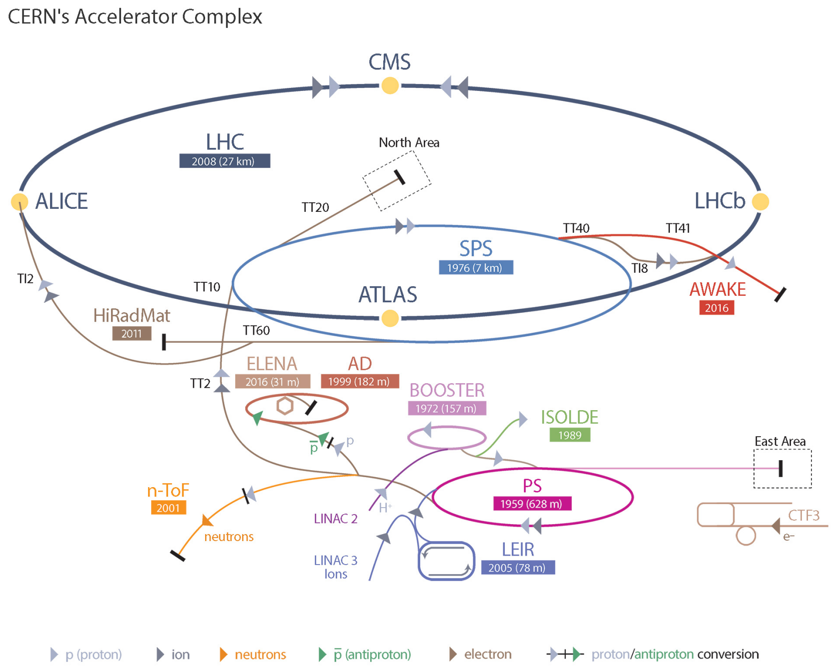

Figure 2.2. Chain of accelerators feeding into the LHC

CMS detector produces a 4 Tesla magnetic field throughout most of the detector. As charged particles move through the magnetic field, their paths curves. The Silicon Tracker allows us to measure the curvature of the path and find their momentum. Next is the Electromagnetic Calorimeter which is mainly responsible for measuring the energy of photons and electrons that result from the collison. Then there is the Hadron Calorimeter which is responsible for detector hadrons, which are particles made up of quarks, such as protons neutrons and pions. These calorimeters work by covering the possible directions out of the collision with scintillator tiles. When the particles hit these tiles they lose some of their energy depositing light proportional to the energy of the particle. The particle will eventually stop having lost all of its energy giving us a reading on its total energy. Finally, are the muon chambers. Muons are interesting particles because while they are heavy particles that will decay they have long enough lifetimes to make it through the detector. In addition, they tend to not be stopped by the detector like the two prior calorimeters almost always stop the particles they detect. Since there is a magnetic field encompassing the detector and the muons have a charge they will curve as they pass through the muon chambers. While not completely stopping the muons will give a reading in the chambers showing its path of travel. By measuring the curve of this path of travel we can measure the momentum. By combining the the data from all the different sub detectors we can get a picture of almost all of the particles that came out of the collision. There are exceptions such as neutrinos which tend to pass through anything leaving no trace. Nevertheless we are able to use this to recreate what exactly came out of the collision, which allows us to find evidence of particles like the top quark which decays so quickly it does not even make it to the detector.

The CMS detector is designed to detector particles coming out of the proton-proton collisions supplied by the LHC. As many different types of particles come out of these collisions the CMS detector is split up into several different sub-detectors. Going from the closest to the collision point outward, first is the Silicon Tracker. The Silicon Tracker is capable of finely measuring the path of the particles that go through it. The CMS detector produces a 4 Tesla magnetic field throughout most of the detector. As charged particles move through the magnetic field, their path curves. The Silicon Tracker allows us to measure the curvature of their path and find their momentum. Next is the Electromagnetic Calorimeter which is mainly responsible for measuring the energy of photons and electrons that come out of the collision. Then there is the Hadron Calorimeter (HCAL) which is responsible for detector hadrons, which are particles made up of quarks, such as protons neutrons and charged pions. The HCAL works by covering almost all of the directions out of the collision with scintillator tile. When particles go through the scintillator tile they interact with the molecules exciting them while the particles lose some of their energies. The molecules in the scintillator will then return to their original energy state emitting a photon. These photons are gather by an optical fiber. By counting these photons we can measure the energy lost by the particle. The detector has enough scintillator tile in the path of the particle to make it highly probably the particle will lose all of its energy in the detector. While this is still a simplification of the process counting the number of photons from the scintillator tile is the basis of the measurement of the energy of the particle. Finally, are the Muon Chambers. Unlike other particles the muon tends to just go through the scintillator only losing a small portion of its energy. This means the muons will reach the last section of the detector mostly unperturbed. Since the muons are charges their path will be curved by the magnetic field so their momentum is measured by a process similar to that of the Silicon Tracker. An illustration of the of the different sub-detectors and the particles that will interact with them is shown in figure 2.3.

Even with all of these sub-detector there are still particles not directly detected. Neutrinos for example tend to go through everything without interacting, and they do not appear in our detectors signals. Several of the particles on table 1.1 decay before ever reaching the detector. To find evidence of these particles we have to find indirect evidence of them. For example, the top quark nearly 100% of the time decays into a bottom quark and a W boson. The W boson then either decays into a charged lepton neutrino pair or a light quark anti-quark pair. By finding evidence of these particles in close proximity we can deduce these came from a top quark.

2.2.1 Hadron Calorimeter

One of the main jobs of the calorimeter is to measure the energy of the of the incident particle. When the particle hits the scintillator tile in the HCAL it interacts with the molecules in the tile exciting them to a higher energy state. The molecules will return to their original energy state emitting a photon. This photon, which is usually blue, will travel through a wavelength shifting fiber around the edge of the tile, as shown in figure 2.4. The fiber will shift the photon into a green wavelength keeping it from exiting the fiber. After traveling through the fiber the photon will enter the

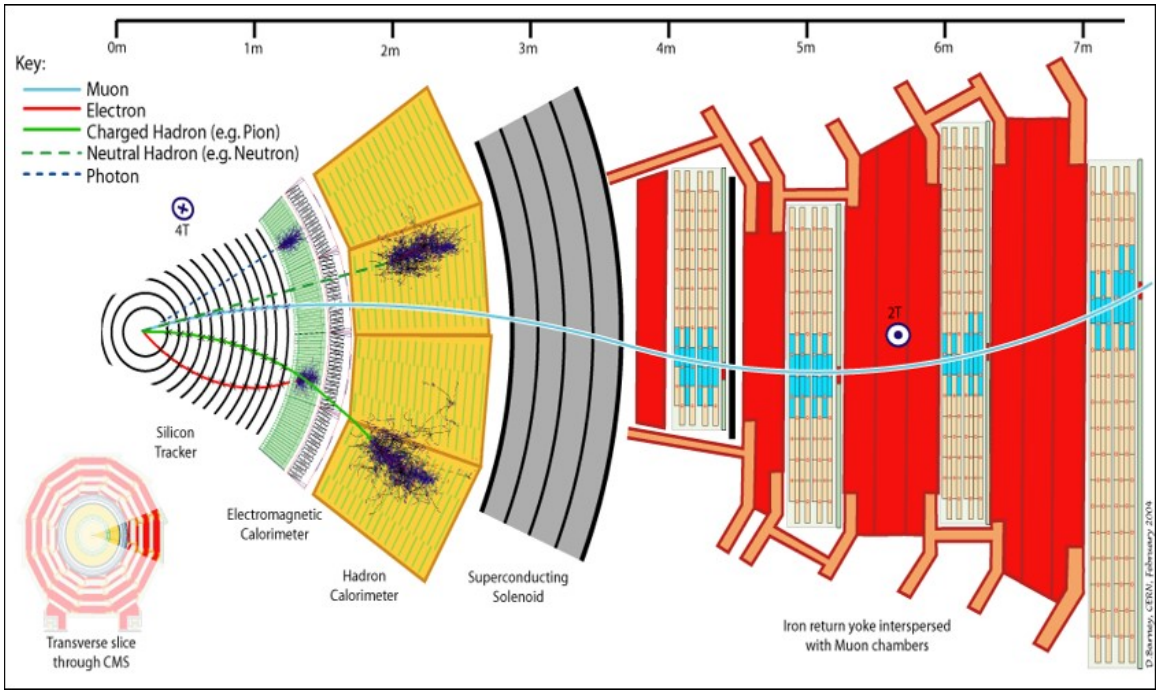

Figure 2.3. A slice of the CMS detector highlighting the different sub-detectors and showing different particles and where they are stopped

Y11 light mixer. This device will collect the light from multiple fibers, mix them, and send them to the photo detector, ensuring consistent and even distribution of the light. The original photo detector for the HCAL was the hybrid photo-diodes (HPD) but they are being replaced by silicon photomultipliers as apart of the upgrades on the CMS detector [3]. When the light is sent to the photo detector it will output charge proportional to the number of incident photons. Because of the nature of the particle's interaction with the scintillator tiles, the number of incident photons is proportional to the energy the particle lost in the tile. The particle will usually not loose all of its energy in a single tile, but the detector is thick enough to ensure most particles will loose all of their energy before making it past the detector.

There are three main section to the HCAL. There is the Hadron Barrel (HB) [4], which surrounds the beam-line like at the edge of a cylinder, the Hadron End-cap (HE), which caps off the cylinder made by HB. These two parts make a cylinder

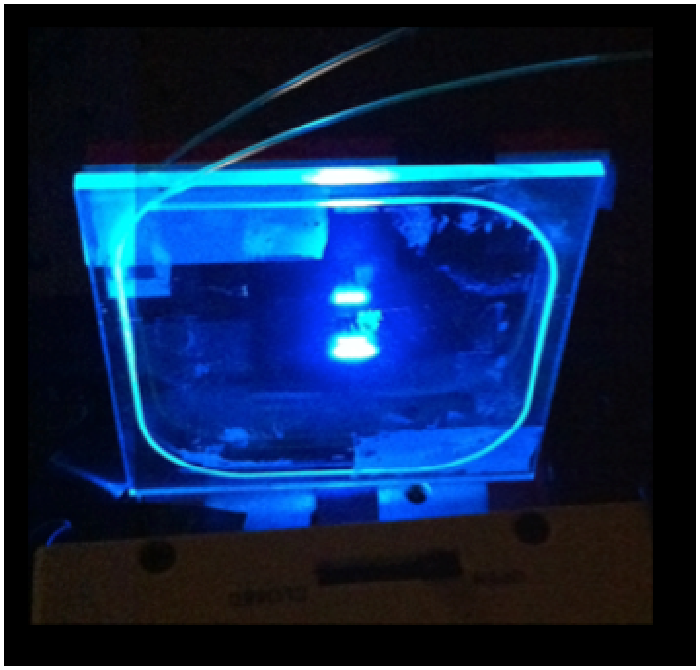

Figure 2.4. A picture of a scintillator tile with the optical fiber around the edges.

which houses the beam-line going through the center and the collision point in the center. Lastly there is the Hadron Front-cap (HF) which is shaped like the HE but is located much further away from the collision point [5]. To describe the geometry of the detector we use a coordinate system related to spherical coordinates with the origin being the collision point and polar angle of 0 being along the beam-line. Phi is the azimuthal angle and Eta is related to the polar angle by $\eta = -\ln(\tan(\theta/2))$ which gives a value of 0 perpendicular to the beam-line and $\pm\infty$ along the beam-line. Usually these coordinates are arranged into discrete integer values denoted iphi and ieta, which are arranged such that a scintillator tile covers one ieta and one iphi as shown in figure 2.5 but there are exception to this. For the distance from the beam-line depth is used which is also a discrete value but there are often more than one scintillator tiles in a single depth.

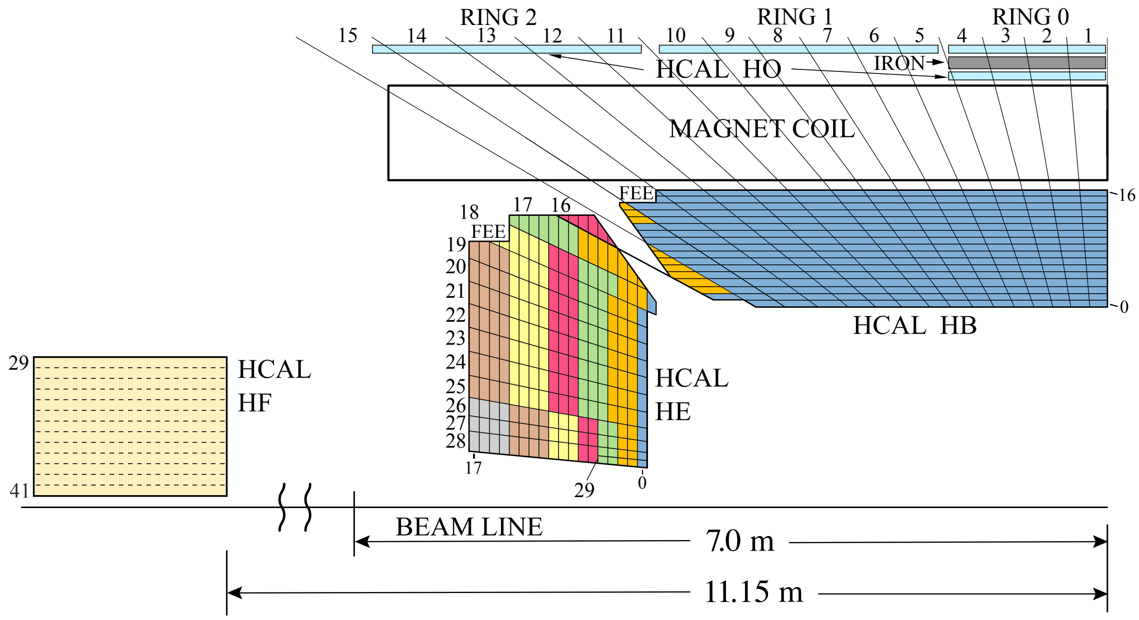

Figure 2.5. Layout of the HCAL showing a single iphi slice of HE HB and HF. Each box represents a scintillator tile

2.2.2 Silicon Photomultipliers

The SiPM does its job of counting the photons from the scintillator by shining them on a pixel face. This is a circular array of really small pixels. A picture of the SiPM is in figure 2.6 showing several pixel faces. There are about 33,000 pixels on a 3.3 mm diameter pixel face. When an individual photon hits one of the pixels on the pixel face it causes a capacitor to fire off a particular amount of charge. The total output charge of the SiPM is the sum of all of the pixels output charge. Theoretically one just needs to sum up the total amount of output charge of the SiPM and one can count the number of incident photons since each pixel will fire off a set amount of charge. Counting of the number of incident photons will give a measurement of the incident particles energy. There are some things that complicate the SiPMs readings. SiPMs are non-linear devices, meaning the total output charge of the SiPM does not necessarily increase linearly with the number of incident photons. In fact, experiments have shown that graphing the number of incident photons vs. the SiPM output charge it looks more like a square root function rather than a straight line. At low incident photon count on the order of 1,000 photons the SiPM is very close to a linear device but as the incident number of photons increases the output charge does not increase at the same rate. There are several factors that contribute to SiPM non-linearity but the two main ones are cross talk and saturation. Cross talk is when a pixel is activated by a photon there is a chance that this activated pixel could activate some of its neighboring pixels artificially increase the output charge of the SiPM. When the photon hits a pixel it excites an electron causing an electron cascade and charge to flow. This excited electron has a chance to emit an IR photon which could go in any direction. If it hits one of the neighboring pixels it could activate it just like an incident photon.

Saturation is when a pixel is hit in rapid succession by multiple photons. When a pixel is hit by a photon it discharges its capacitor which is the source of its output charge. After the pixel fires it needs some time on the order of 10 nanoseconds to recharge its capacitor. If the pixel is hit it simply fires off whatever charge it has in its capacitor at the time, which could be reduced from its normal charge. Given that the SiPM has about 33,000 pixels on its pixel face, when the number of incident is on the order of 1000 this effect is insignificant, but particles can produce much more photons where this effect can be much more significant. The non-linear properties of the SiPM makes it a bit harder to get accurate measurements, but there are ways to study them which will allow us to compensate for these affects.

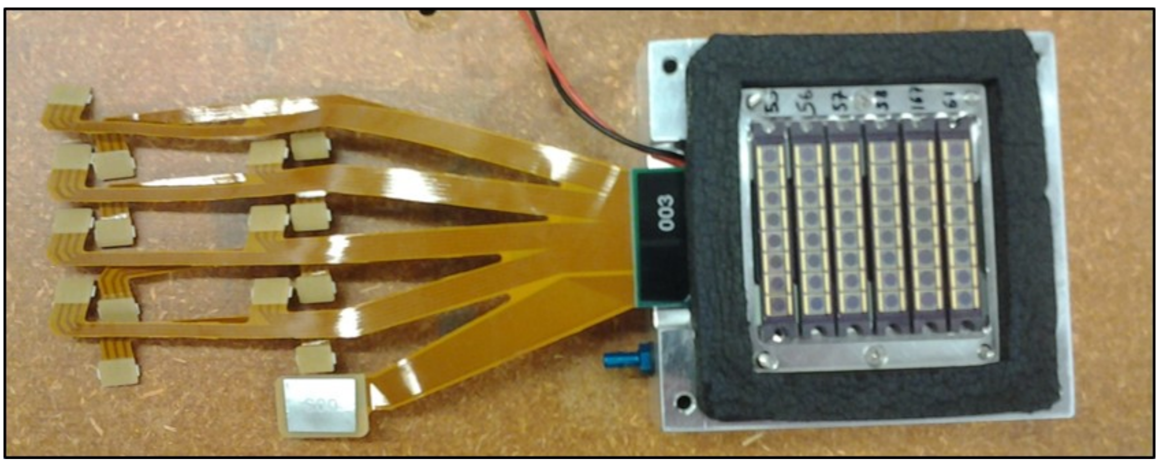

Figure 2.6. A picture of a Silicon Photomultiplier

CHAPTER THREE

Test Beam

3.1 Test Beam Setup

The new readout modules being installed in the CMS detector have several new components such as new charge integrator and encoder (QIE) chips, but the main subject of my work was the SiPM. To study the features of the SiPM such as non-linearity, we used a test beam. The test beam is a linear particle beam that comes from the SPS accelerator when it does not feed into the LHC. The particles from this beam are not at the energies of the protons in the LHC but they are much easier to make and control. There are several different experiments that use this beam but the HCAL has a mock test stand that can be moved into the path of the beam when experiments need to be run. The CMS detector is 100 meters underground and is in a cavern that, due to radiation and tight enclosures, makes the detector difficult to access. Though modifications and maintenance can be made during shutdowns this is not the ideal way to perform tests on new electronics. The test stand at the test beam location called H2 is on ground level and can be easily accessed. In addition the energy and particle type of the beam can be easily controlled. The test stand is designed to be similar to a portion of the HCAL on CMS. Using this test beam we can shoot particles like pions at the test stand, which has the new readout module installed and look at the response [6]. We can vary the energy of incident particles which should increase the number of photons produced in the scintillator tiles. This means there will be more input photons on the SiPM.

Because we are looking for statistical significance in the data we need to gather a lot of data. This means we take runs with several thousand events or particles hitting the test stand and take several of these runs to ensure high statistics. Because we

Figure 3.1. A picture of a the test stand at H2. The scintillator tiles are covered in the black tedlar and the new readout modules are connected in the back. The stand can be shifted so the beam can be aimed at different sections.

will be taking data over a long period of time, we want to ensure that we record data only when a particle is hitting the test stand. One of the key systems that helps this is the trigger system. In the path of the beam before the test stand we put scintillator tiles in order to send a generic signal to the control room. A total of four tiles were placed in the path of the beam. When we saw signals from these tiles we know that a particle is coming from the beam. This serves as a trigger signal for our data acquisition system. The trigger signal then goes to the back-end electronics that stores the data from the detector. In this way we only store data around the time when we know a particle is hitting our test stand. There is also a ready signal that goes from the back-end electronics to the trigger. Since a particle may come before the back-end electronics are finished storing the relevant data, a trigger signal that comes without the ready signal will simply be ignored.

Although built to be similar to the HCAL on the CMS detector, the test stand is smaller and has some differences. When looking at the data from the teat beam, it is important to be sure that the e-map, which traces the channels that receive the data to the actual scintillator tiles on the detector, is correct. There are some differences in this map from the test stand and the H2 control room and the HCAL detector and the CMS experiment cavern. In order to account for these differences a new emap was created for the test beam setup. With an accurate e-map we can create an accurate picture of the incident particles hitting the test stand. The test beam allows us to control the energy and type of particles incident on the test stand. This allows us to study things like SiPM non-linearity as we can look at the output of the SiPMs under something like 50 GeV pions then increase to energy to something like 150 GeV and compare the different responses. However the particle does not deposit its energy in a single scintillator tile. For something like a pion, it will lose a part of its energy with each scintillator tile it hits and eventually be stopped by the detector, but its total energy will be spread throughout the detector. Since each particle in the beam has roughly the same energy and we can isolate the event of a single particle hitting the detector we are to find energy lost in each scintillator tile but looking at the complete picture of the detector.

SiPM non-linearity is not the only thing that is being researched using the test beam. In the CMS detector, particles come so fast that the signals of individual particles blend together. In the test beam, the particles are more spread out so it is easier to isolate the signal of individual particles. This makes it easier to extract the pulse shape of the readout modules which is the shape of the output charge vs. time. It is also important to see if the pulse shape changes significantly under different circumstances such as higher or lower energies. Using the pulse shape of the readout modules we can then extract the individual signals in the CMS detector.

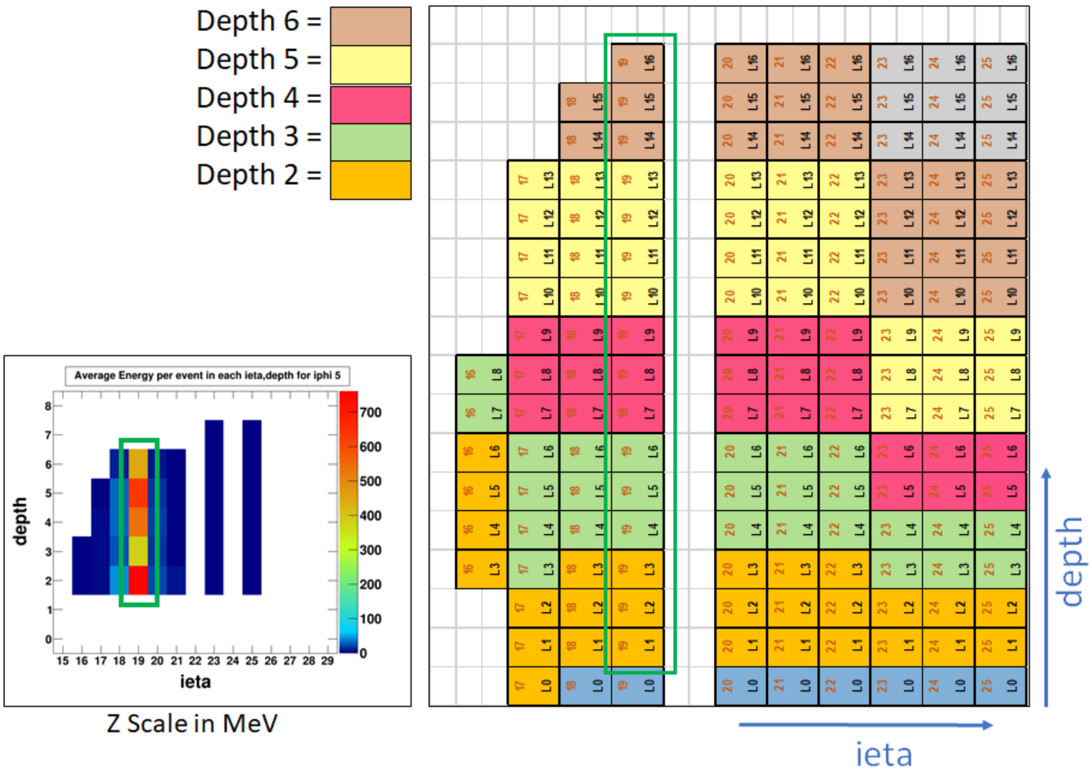

Figure 3.2. This shows the relationship between the emap on the left showing which contains a geometric layout of the scintillator tiles in a single iphi slice and the data plots in a run with 150 GeV muons.

3.2 Test Beam Analysis

With a proper e-map, we can get a picture of the incident particle, observe its path, and see where it deposited its energy. Since the particle does not deposit all of its energy in a single scintillator tile, this is critical when trying to recreate the particle energy. It is also important that there are often a variable amount of scintillator tiles in a single depth channel as shown in figure 3.2 which shows 4 scintillator tiles in depth 5 and 3 scintillator tiles in depth 4. Looking at the results in the plot to the left, it explains why there is more energy deposited in depth 5 rather than depth 4.

Muons are useful for many things, but when trying to recreate the energy of the particle, it is easier to use pions. The reason for this is that muons tend to go through the detector depositing a small portion of the energy but not being entirely

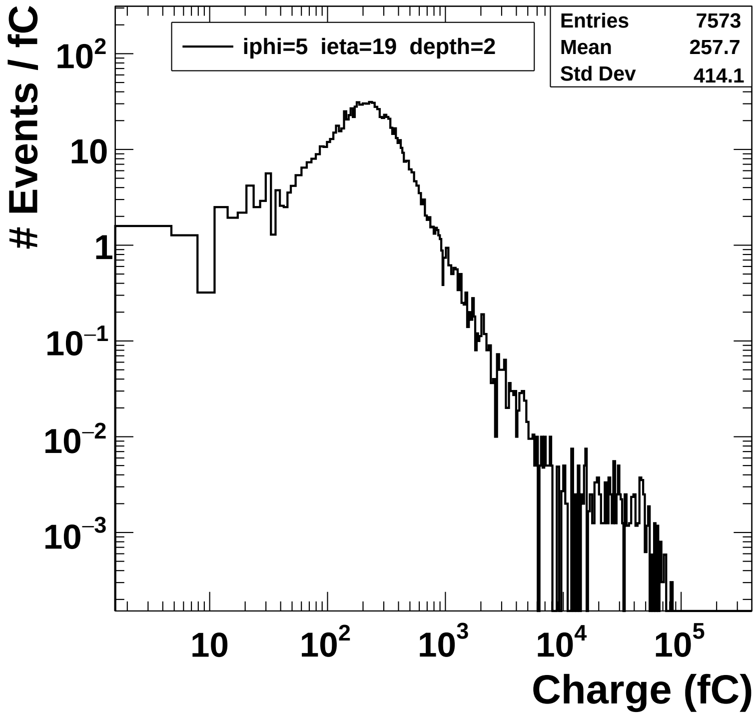

Figure 3.3. A plot showing the number of events that output a certain amount of charge. This run used 150 GeV muons.

stopped. This can be seen in figure 3.2 which shows the muons depositing a consistent amount of energy in each of the depths even the far ones. Figure 3.3 shows that the majority of the events in this muon run produced several hundred femtocoloubms in a single channel of the detector. Trying to recreate the energy of the incident muon would not give the actualy energy, as it would be significantly less than the actual energy of 150 GeV. On the other hand figure 3.4 shows a plot with a pion run. This shows that the pions hit the scintillator tiles in depth 2 depositing a large portion of their energy and depositing less and less in the subsequent depths with basically nothing in the last depth. There is also more significant spread compared to the muon run which shows the muons going straight through while the pions leave some energy in the neighboring channels.

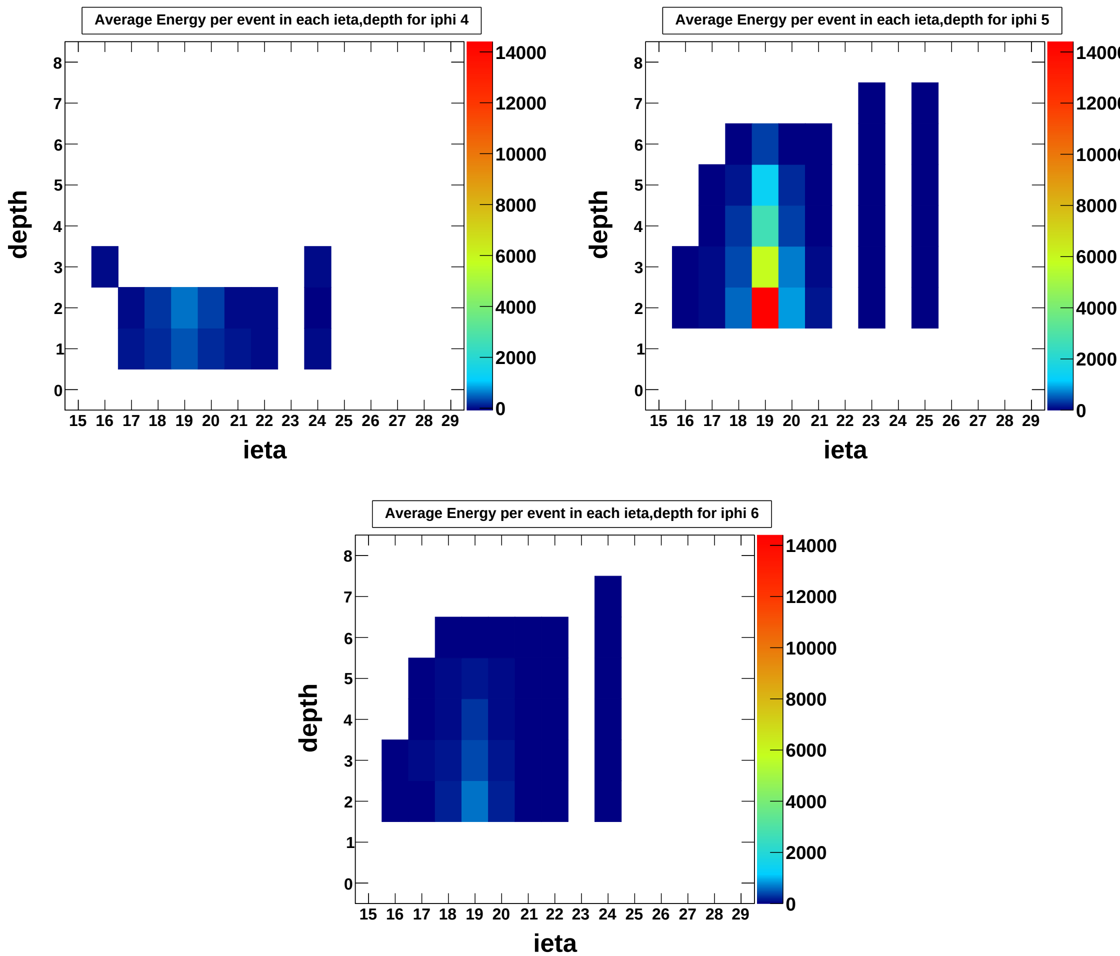

Figure 3.4. These plots show the recreation of an event with 50 GeVpions showing the pions aimed at iphi 5 ieta 19 and the energy deposited in each channel z scale in MeV. The different plots show different iphi locations.

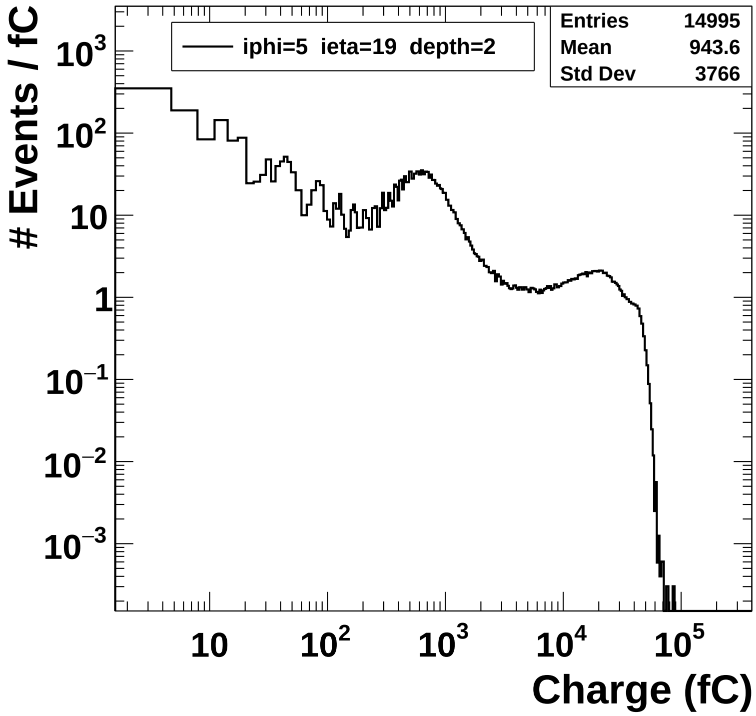

Figure 3.5. This shows the number of events that produces output charge in the SiPM. The peak in the middle shows the average output charge in response to the incident particles at this energy.

To recreate the energy of the incident particle we can look at plots such as figure 3.5 which shows the mean output charge in a 50 GeV pion run. By looking at this output charge and the output charge of the other channels, we can find what portion of the particles' energy was deposited in this channel and then going by the known energy of the particle how much energy was deposited to produce this output charge.

The output charges of the different events can be shown in figure 3.6 which shows the number of events that output a certain charge. This figure can also be used to start the analysis on the SiPM non-linearity. One key thing about the non-linearity is that at low charge output and correspondingly low particle energy the SiPM is very near linear, and it is only at high output charge does this effect become significant. This means to study non-linearity one needs to use particles at sufficiently high energies. After the test beam was over and the analysis of the data was started it was discovered that the test beam was not really capable of producing particles at energies in the non-linear range of the SiPM. To illustrate this looking at figure 3.6 it is apparent that in the 300 GeV run, an energy close to the maximum the test beam is capable of producing, there are minimally few events that output charge above 300,000 fC. The SiPM outputs approximately 40 fC for every incident photon electron which means the highest energy events create about 6000 incident photo electrons. When using a simulation of the SiPM it is apparent that this is still very much in the linear range of the SiPM. One thing to note is that not all of a single particle's energy goes to a single SiPM. In figure 3.5 is shows that while the majority of the particle's energy is deposited in the first group of scintillator tiles it hits there is still a signficant portion that is in neighboring channels. Summing over all the channels should give the total energy of the particle but this means that 300,000 fC does not directly translate to 300 GeV. As the energy of the particle increases its energy will spread out more which means a 600 GeV pion will not necessarily deposit 12000 photo electrons in the first channel it hits.

One of the key things in doing a pulse shape analysis using test beam data is the timing information. In the test beam, we take two different timing information. The first comes from the QIE chips in the readout modules. The readout modules measure the output charge of the SiPM over 250 ns, and the information is binned into 10 time samples each 25 ns long. The output pulse of the SiPM is about 75 ns long, and it usually stays confined to 3 or 4 time samples. In addition we also take what is called a Time to Digital Converter (TDC) value. This value stores at what time in the 250 ns span the output charge of the SiPM crossed a threshold with a 0.5 ns resolution. Since the output charge starts out below this threshold, the TDC value should give the start of the output pulse of the SiPM. For instance, a TDC

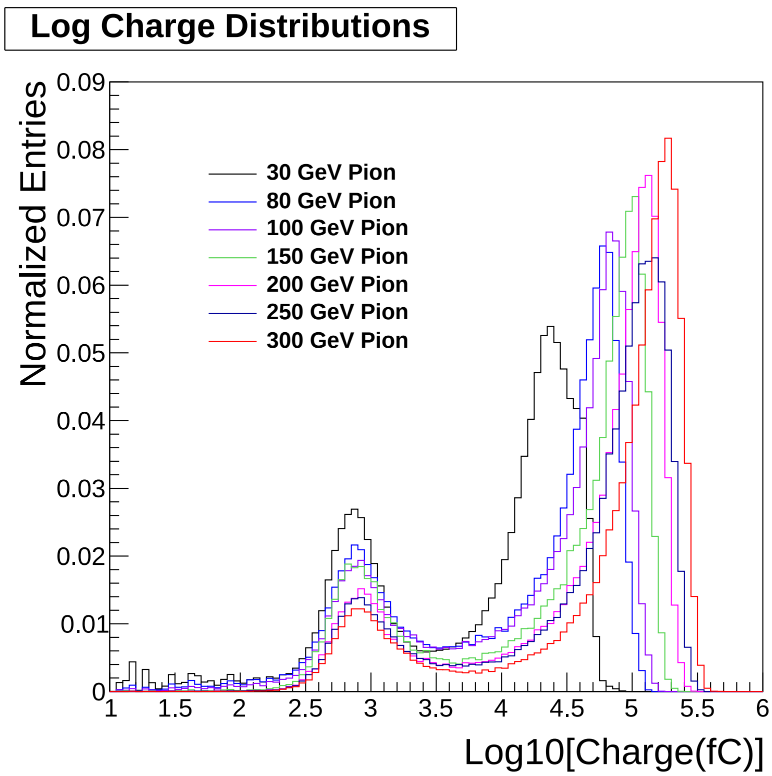

Figure 3.6. A plot showing the charge output of the different events over the different runs used to find the pulse shape.

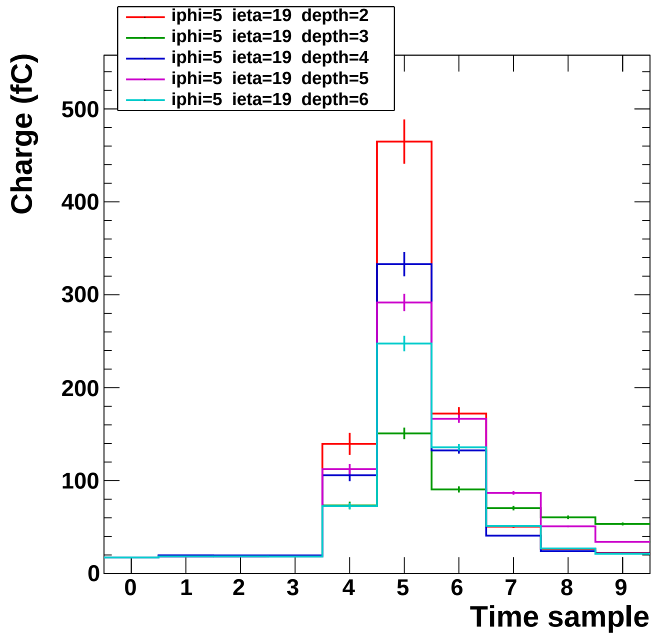

Figure 3.7. A histogram of the output pulse of the readout modules binned in 25 ns bins. This is from a run with 150 GeVmuons aimed at iphi 5 and ieta 19. This plot shows the output pulse of the different depths at that location.

value of 20 in time sample 4 means the pulse crossed the threshold charge value 10 nanoseconds after the start of time sample 4 or 110 nanoseconds after the start of data taking. One of the problems with the TDC value is that it could be affected by the amplitude of the output pulse as a high amplitude will cross this threshold earlier. To extract the pulse shape we can do something called a phase scan.

When we take a run using the test beam, we do not just take data from one single particle but several thousand stored in their own individual events. For instance, when we took a run with 250 GeV pions that the run has several thousand events recording the data when the particles all at about 250 GeV hit our test stand. Because of the nature of the test beam and also just quantum mechanics there is some randomness to each event. To do a phase scan we take advantage of this randomness by looking at pulses with the same total charge but different TDC values. Theoretically, two pulses with the same charge but different TDC values should be

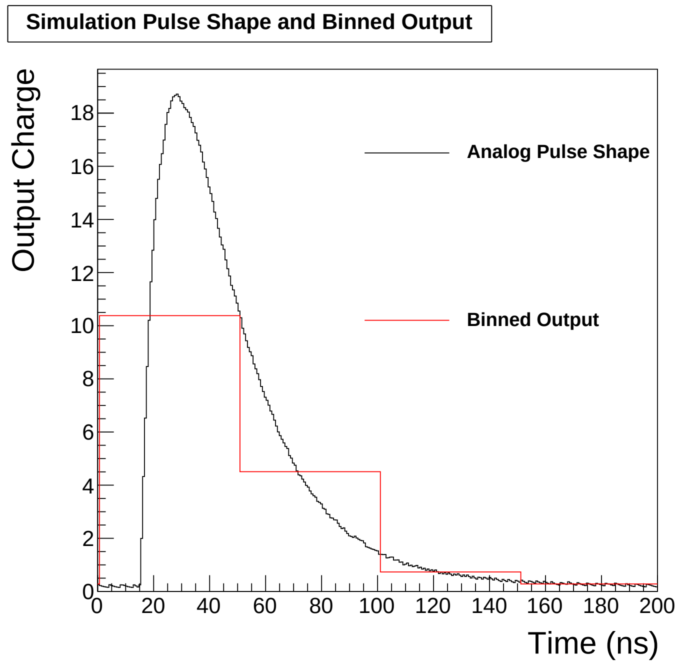

Figure 3.8. A plot from a SiPM simulation showing an analog version of the output charge along with the same output binned in 25 ns bins.

exactly the same except for a time shift. These pulses could look different in data though as different parts of the pulse will be put into different time samples. Figure 3.8 shows an analog pulse shape along with its binned output. A phase scan takes the difference in binned pulse value from several different pulses all with similar overall charge but a range of TDC values. Figure 3.9 shows multiple sets of data all with different TDC value illustrating how changing the TDC value can change the bins without changing the total output charge. An example of this is taking the difference of the charge value from time sample 4 in a pulse with a TDC value of 20 also in time sample 4 and the charge value from time sample 4 in a pulse with a TDC value of 21 also in time sample 4 gives the pulse height at nanosecond 110 in the 250 nanosecond long data set. Doing this process over all the time samples with more pulses with TDC values ranging from 0-49 all in time sample 4 will give a more analog version of the pulse shape as shown in figure 3.10.

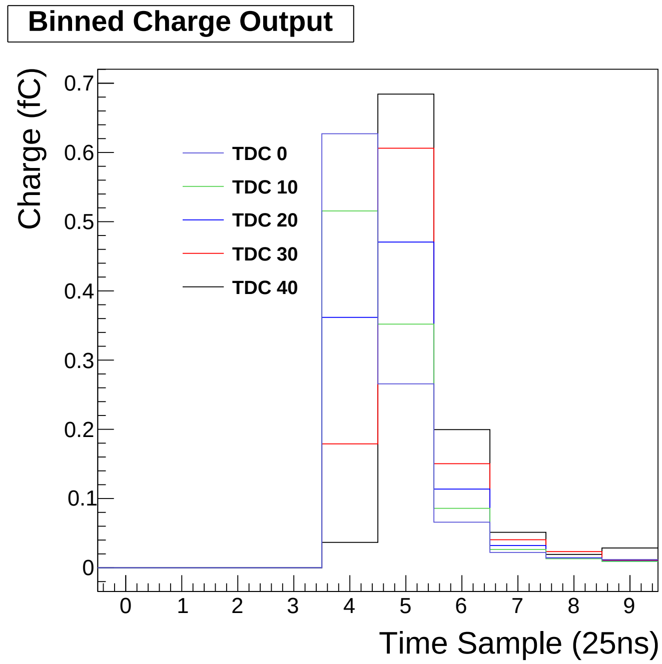

Figure 3.9. A plot showing the binned output charge of events with different TDC values. All pulses have their TDC value in time sample 4 and have a total output charge in the range of 50,000-80,000 fC

There is also the trigger information. This timing information comes from the test beam equipment that signals the back end electronics to store the data from the readout modules. The trigger information theoretically does not have the same discrepancy as TDC information, but most people still use the TDC from the QIE chips. The relationship between the two signals can be shown in figure 3.11. Theoretically this timing information could be used for a phase to obtain an analog pulse shape like that in figure 3.10.

To do a phase scan properly, we need to use events that have similar output charge. There are a variety of reasons for this, but one of them is that there is evidence that the pulse shape may change with output charge. To study this we simply have to do a phase scan using event with different output charge and see if there are any significant changes. Although the particles will have about the energy the test beam is set, to it is common to have several outliers. To minimize this disturbance we take

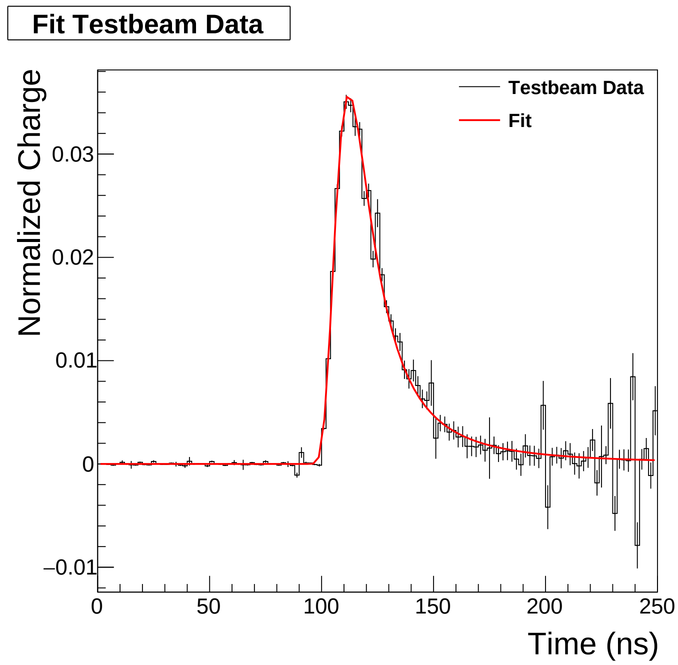

Figure 3.10. A plot showing a more analog version of the SiPM pulse shape obtained using a phase scan on test beam data. It is also fitted by a Landau Gaussian function which is what we expected from theory. The total output charge of the runs used in this range from 10,000-29,000 femtocoulombs.

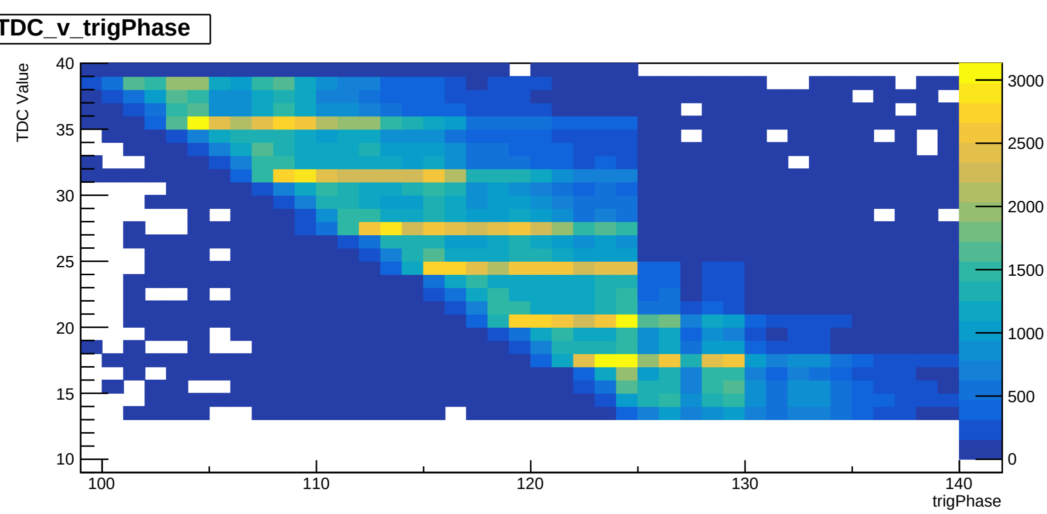

Figure 3.11. A histogram showing the statistical relationship between the trigger timing information and the QIE TDC information.

in all the events from several different runs energies ranging all the way from 30 GeV to 300 GeV and only use the events that fall within a certain charge range. Figure 3.12 shows pulse shapes obtained using several different charge ranges. Figure 3.13 shows the fits of these pulse shapes overlapping for comparison purposes. The fits show that there is little change of the pulse shape as the charge increases but there is a small trend visible in this plot. Looking at the peak of the pulses it is apparent that the lower charge pulses have shorter peaks. This lack of area is made up in the second half of the pulse as the lower charge pulses are slightly higher there though this is harder to see as it is over a longer period of time. This result is not unexpected as the non-linearity of the SiPM can shift the charge of the pulse towards the front.

3.3 Conclusions

Using the test beam data we were able to extract a precise pulse shape of the new readout modules. This pulse shape does appear close to expectations and have a reasonable to the Landau Gaussian function. The pulse shape does show minor changes with changes in the output charge but at the energies from the test beam there was very little changes. The non-linearity of the SiPM was not able to be studied in depth using the test beam data, but we were able to confirm that at energies from the test beam the SiPMs are very close to linear. These readout modules were installed in the HE on the CMS detector over the winter of 2018.

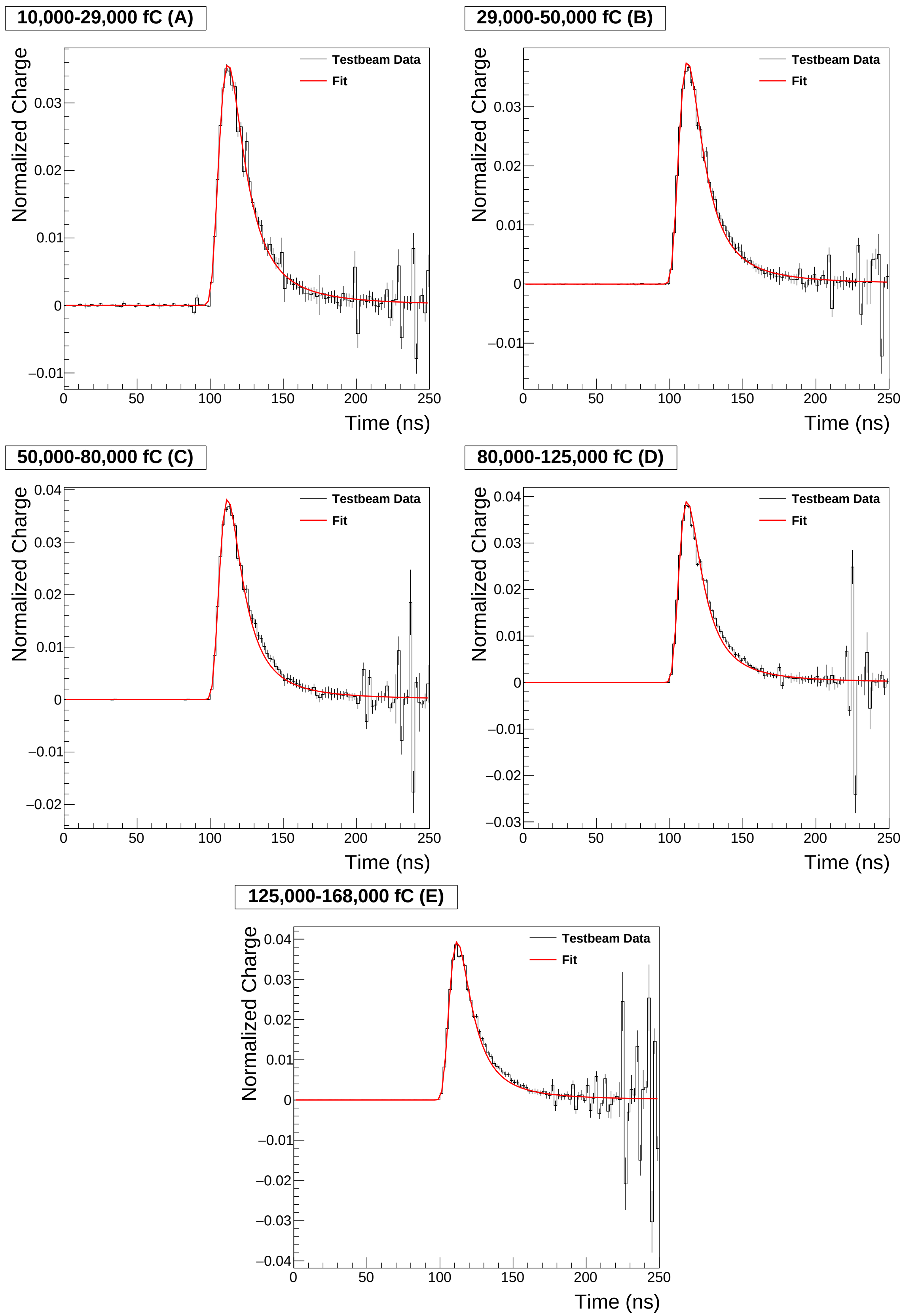

Figure 3.12. Fitted pulse shapes of using events of charge 10,000-29,000 fC (A) and 29,000-50,000 fC (B)

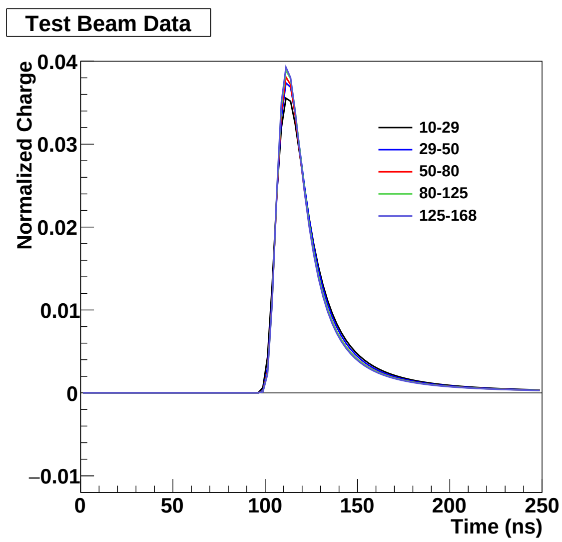

Figure 3.13. The comparison of the fits to the pulse shapes.

CHAPTER FOUR

SiPM Simulation

4.1 SiPM Simulation

In addition to studying the new electronics with the test beam, we also did some work wtih a SiPM simulation which could use theoretical signals from the detector and give the SiPM's response to them. When the light from the detector goes to the SiPM a Y11 light mixer is used so that the light is spread across the pixel face. The light mixer has a unique shape, shown in figure 4.1 in which it shines the light onto the pixel face. Using a mathematical representation of this pulse shape we can simulate how light is shined on the pixel face. We can then create a virtual pixel face that has accurate geometric representation. Each of these virtual pixels could be activated by the incoming Y11 light pulse and would respond by firing off a set amount of charge as would an actual SiPM. When these pixels are activated they also have a certain probability to activate a neighboring pixels which will simulate the cross talk of the SiPM. Each pixel also has a recharge rate such that if hit in rapid succession it will fire with a reduced amount of charge emulating the saturation effect. Using this simulation we easily adjust the number of input photons and get very good details of the SiPM response. We can also easily turn different things off to see how significant individual effects are. This simulation is capable of producing more fine tuned data and in greater quantities than test beam data. In addition, it is able to simulate situations that are not possible in the test beam. On the other hand the accuracy of this simulation is heavily dependent on the data we input into it.

Since the program can simulate the non-linearity effects of the SiPM, we can use theoretical inputs to the SiPM to study its effects. The light a particle deposits in a scintillator tile can vary in time the Y11 light mixer ensures that the input light

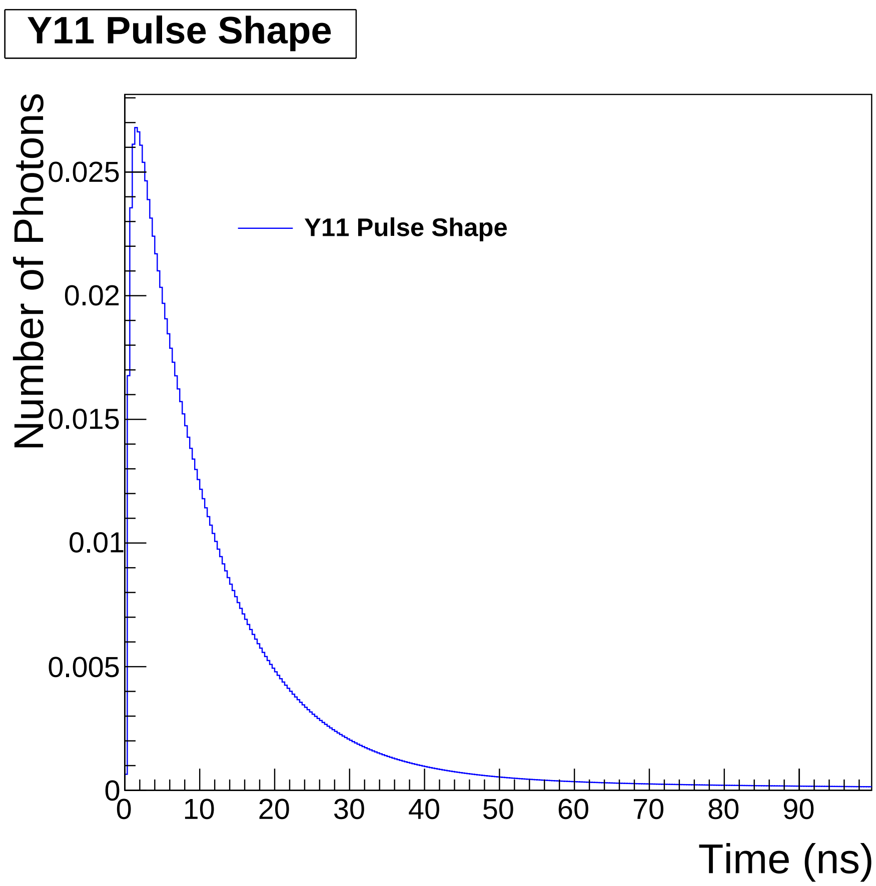

Figure 4.1. A graph of the Y11 pulse shape with nanoseconds on the x axis and number of incident photons on the y axis

pulse shape remains constant. This means to change energy of the incident particle we just have to increase the number of photons in the input pulse while keeping the same shape. The output of the virtual SiPM is normalized so if the simulation was a completely linear device its output ”charge” should exactly equal the number of input photons.

4.2 Simulation Analysis

To do the analysis using the SiPM simulation, we simply measure the total output of the SiPM over a light pulse and compare it to the number of input photons. Since there is a degree of randomness we will use the average pulse over several inputs. Compared to using test beam data the analysis with the simulation is simple. In test

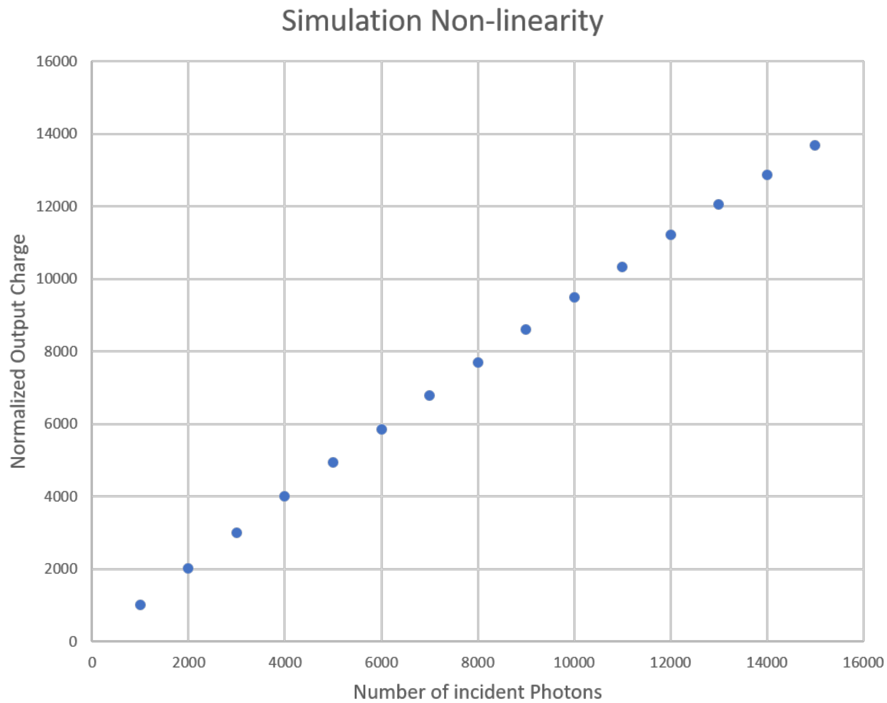

Figure 4.2. Graph of number of incident photons vs output charge of the SiPM simulation. Given the units of the simulation a perfectly linear device would have all data points falling on the y=x line but as shown as the number of incident photons is increased the data points fall short of this line.

beam the energy of the particle is spread over several SiPMs while in the simulation we have a very fine control of the input energy to the single SiPM. With a plot of input number of photons vs SiPM output charge we then create a correction curve that is necessary to make the graph linear. This is process for doing a non-linearity analysis using test beam data so we can compare the two correction curves to see if there is agreement. With other analyses it is common to simply divide out the cross talk. Given that there is a 15.4% chance of crosstalk with a large signal of several thousand photons it is assumed that 15.4% of the signal from the SiPM is due to cross talk so that number is simply divided out. This means the majority of the effects that the correction curve is compensating for is saturation. Figure 4.2 shows the non-linearity obtained from the simulation.

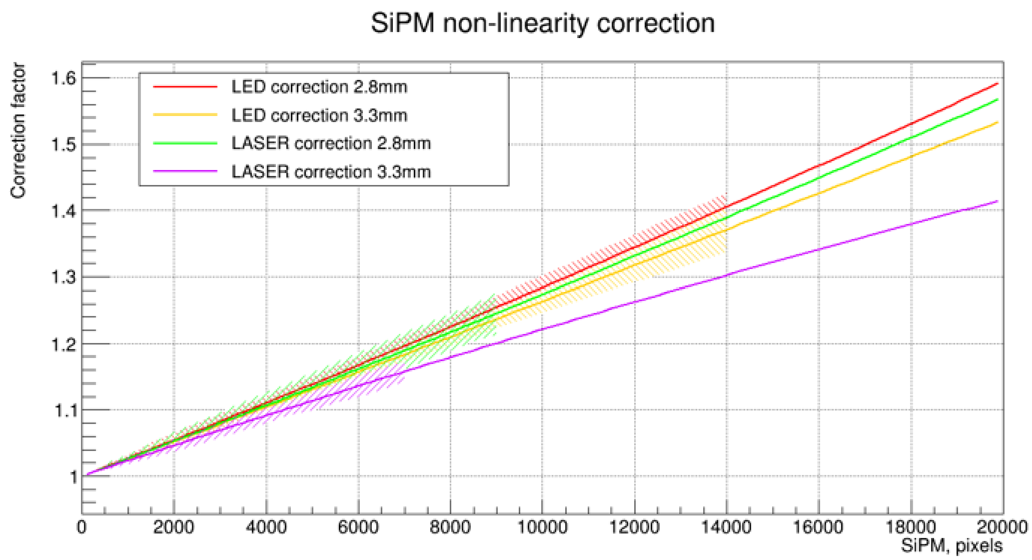

Figure 4.3. Graph of the correction factor vs. number of pixels fired. The correction factor is the number the output needs to be multiplied by in order to obtain the linear output value. This means a perfectly linear device would always have a correction factor of 1. This data was obtained from shining a laser directly on the SiPM.

To be sure the simulation is designed correctly it is useful to compare things like non-linearity to the actualy SiPM. Figure 4.3 shows the non-linearity of the SiPM from shining a laser directly on the SiPM. Figure 4.4 shows a similar plot constructed using the simulation. There is significant disagreement between these two sets of data.

One effect of the saturation that is less understood and harder to implement is that the pixels can sometimes recharge faster. This effect is due to the QIE chips in the readout modules which in addition to taking and processing the charge from the SiPMs also supply the charge that recharges the capacitors for each individual pixel. The capacitors for the pixels recharge exponentially like normal RC circuits. Normally the time constant for the capacitors is about 9ns which means the capacitor is completely charges after 20ns but this is when the SiPM is outputting a very low amount of charge to the QIE chips. When the SiPM is outputting more charge the QIE chips then supply more charge to the SiPM recharging the pixels faster. When

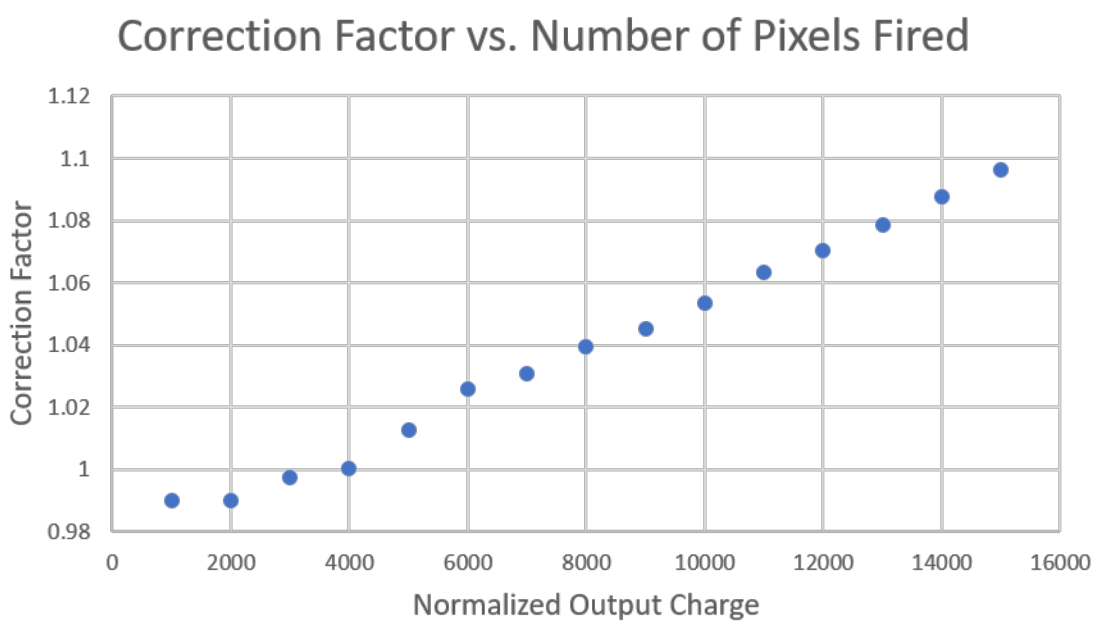

Figure 4.4. Graph of the correction factor vs. number of pixels fired. The correction factor is the number the output needs to be multiplied by in order to obtain the linear output value. This means a perfectly linear device would always have a correction factor of 1. This data was obtained from the SiPM simulation.

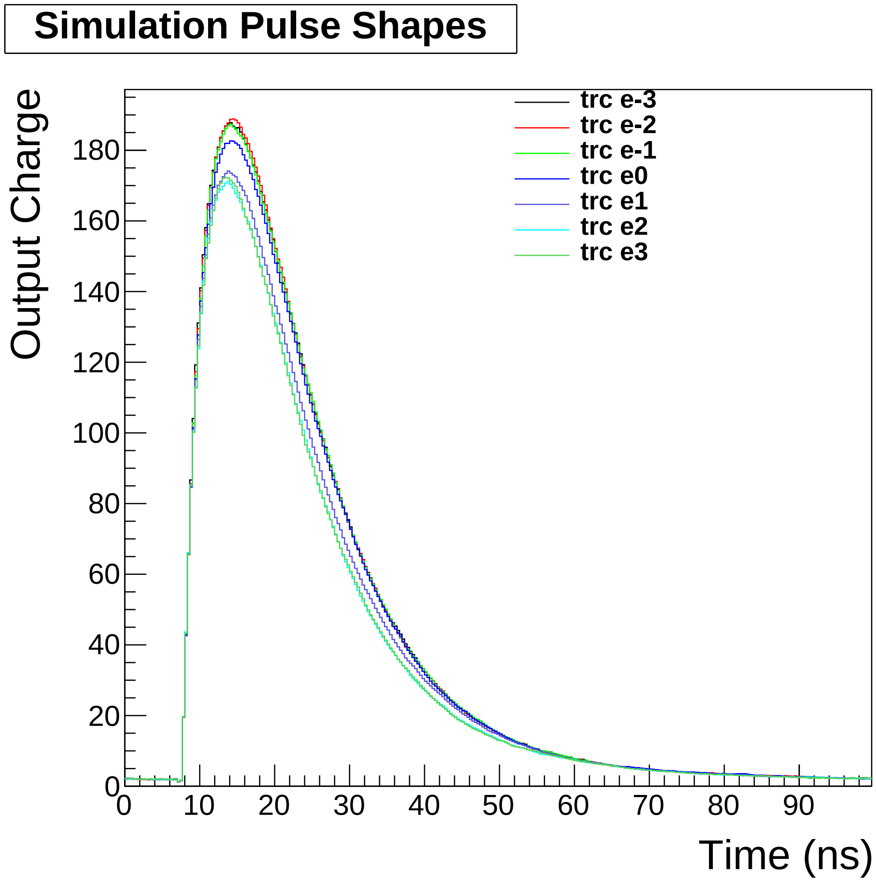

Figure 4.5. Output pulses of the SiPM simulation with 10000 incidents photons comparing the effect of changing the recharge time constant on the pixels. The TRC value is the recharge time constant.

the pixels recharge fast they will fire off closer to their maximum charge even when hit in rapid succession. This means as saturation becomes more prevalent with a high number of incident photons this reduces the effects of saturation. The effect of different recharge time for the pixels can be see in figure 4.5.

Using the simulation we can also look at the pulse shape of the SiPM. This pulse shape should theoretically be the same obtained from test beam data. One of the main things that is necessary to look at is does the pulse shape change significantly with a change in input energy. As shown is figure 4.6 does not significantly change with different energies.

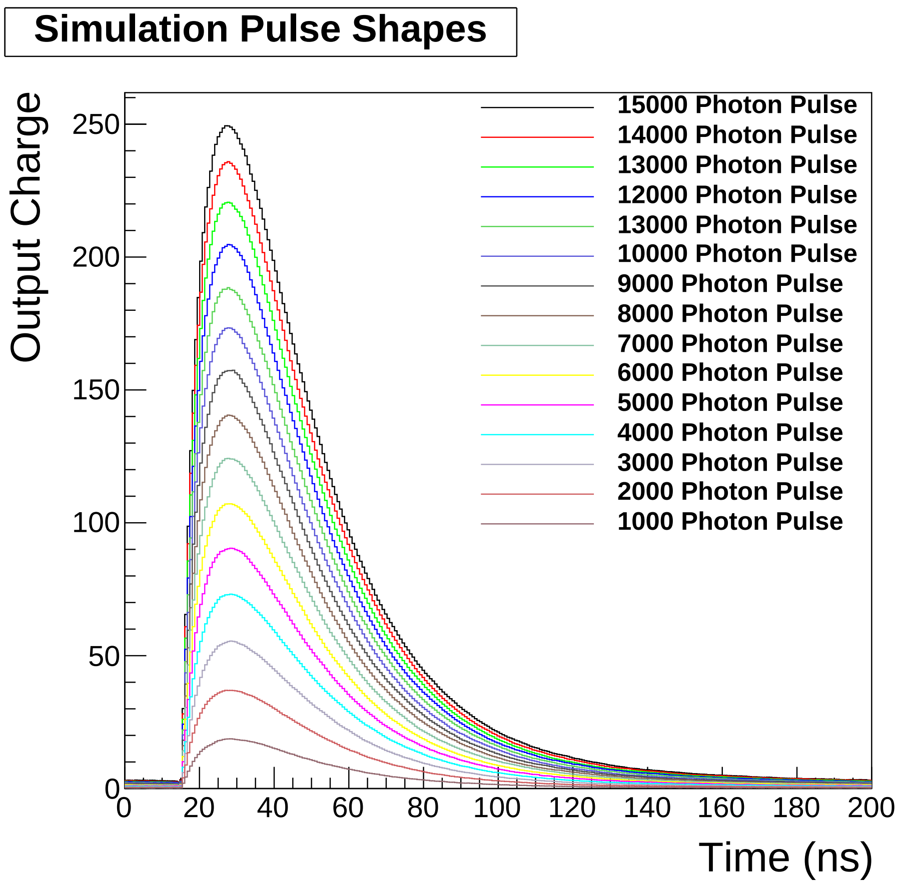

Figure 4.6. Pulse shapes from the SiPM simulation. They are stacked on top of each other to highlight any differences from an increase input photon count.

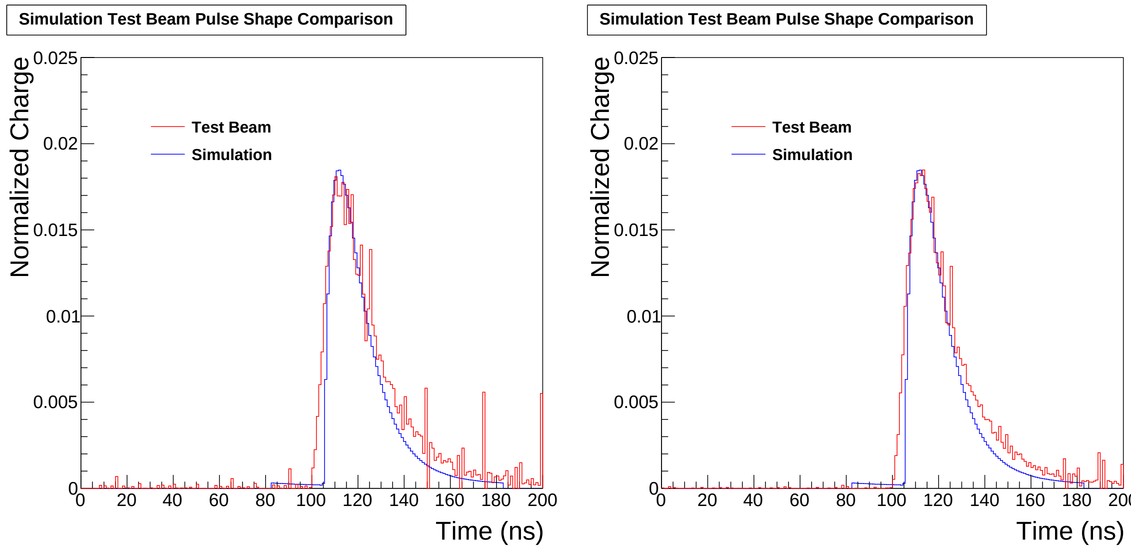

Figure 4.7. Histogram of the pulse shapes from the simulation and the test beam overlapping for comparison purposes. On the left the charge range is 10,000-29,000 fC on the right is 29,000-50,000 fC

We can compare the pulse shape from the simulation to the one obtained from test beam data. Theoretically these pulses should be the same. For comparison we simply plot the two pulse shapes on top of each other and see if there are any major differences. To minimize the interference of other effects like non-linearity we can compare pulses from similar output charge. Using the conversion ratio of 40 fC to 1 photo electron we can compare pulses from the same charge range. For instance, for the charge range 10,000-29,000 fC we compare it a pulse of 500 photo electrons from the simulation. Figures 4.7- 4.9 show these comparisons. While they do have the same basic shape there are some significant differences mostly the simulation is much narrower in the base.

4.3 *Conclusions*

The creation of the simulation was a very helpful tool in understanding the details of how a SiPM works. It is also a very useful illustration for how it work and it can be easily adjust for future modifications. Some of the plots used in this paper

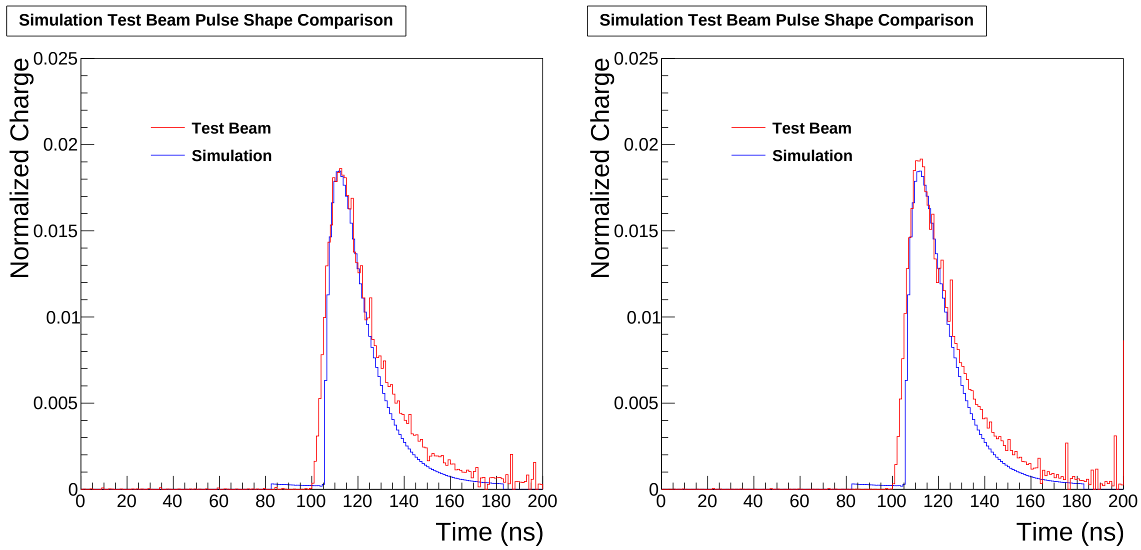

Figure 4.8. Histogram of the pulse shapes from the simulation and the test beam overlapping for comparison purposes. On the left the charge range is 50,000-80,000 fC on the right is 80,000-125,000 fC

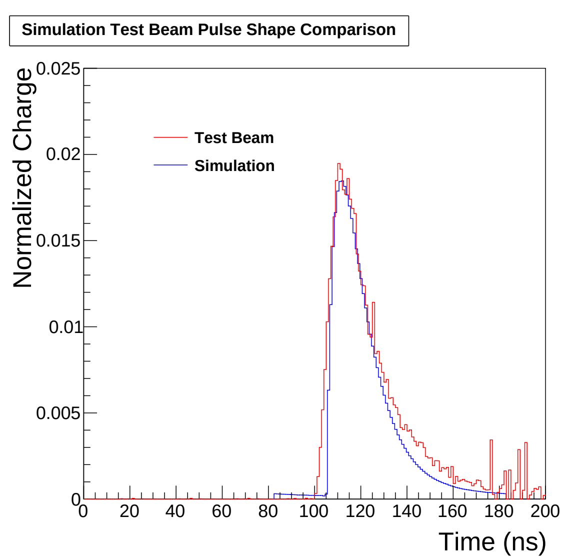

Figure 4.9. Histogram of the pulse shapes from the simulation and the test beam overlapping for comparison purposes. On the left the charge range is 10,000-29,000 fC on the right is 125,000-168,000 fC

to explain how a SiPM works were created using this simulation. The analysis of the simulation, however, shows that there is still some major flaws with the simulation. The pulse shape comparison shows that the simulation shape is significantly narrower in the base than the actual pulse shape. In addition, the non-linearity in the simulation is much smaller than measurements made using an actual SiPM. The reasons for these discrepancies are still being investigated, but there are several leads. Among them are the changing recharge times and other affects such as the scintillator tiles and QIE chips not yet taken into account in the simulation.

BIBLIOGRAPHY

[1] S. Chatrchyan *et al.*, “Observation of a new boson at a mass of 125 GeV with the CMS experiment at the LHC,” *Phys. Lett.*, vol. B716, pp. 30–61, 2012.

[2] S. Chatrchyan *et al.*, “The CMS experiment at the CERN LHC,” *JINST*, vol. 3, p. S08004, 2008.

[3] J. Mans, J. Anderson, B. Dahmes, P. de Barbaro, J. Freeman, T. Grassi, E. Hazen, J. Mans, R. Ruchti, I. Schimdt, T. Shaw, C. Tully, J. Whitmore, and T. Yetkin, “CMS Technical Design Report for the Phase 1 Upgrade of the Hadron Calorimeter,” Tech. Rep. CERN-LHCC-2012-015. CMS-TDR-10, Sep 2012. Additional contact persons: Jeffrey Spalding, Fermilab, spalding@cern.ch, Didier Contardo, Universite Claude Bernard-Lyon I, contardo@cern.ch.

[4] S. Abdullin *et al.*, “Design, performance, and calibration of cms hadron-barrel calorimeter wedges,” *Eur. Phys. J.*, vol. C55, p. 159, 2008.

[5] S. Abdullin *et al.*, “Design, performance and calibration of the cms forward calorimeter wedges,” *Eur. Phys. J.*, vol. C53, p. 139, 2008.

[6] V. V. Abramov *et al.*, “Studies of the response of the prototype cms hadron calorimeter, including magnetic field effects, to pion, electron, and muon beams,” *Nucl. Instrum. Meth.*, vol. A457, p. 75, 2001.